

Intrinsic quantum dots in partially ordered bulk (GaIn)P

U. Kops, P. G. Blome, M. Wenderoth, and R. G. Ulbrich

IV. Physikalisches Institut, Universität Göttingen, Bunsenstrasse 13, D-37073 Göttingen, Germany

C. Geng and F. Scholz

4. Physikalisches Institut, Universität Stuttgart, Pfaffenwaldring 57, D-70550 Stuttgart, Germany

(Received 8 February 1999)

We present a photoluminescence study with 500 nm lateral resolution on partially ordered bulk (GaIn)P alloys at lattice temperatures 3–60 K, external magnetic fields 0–12 T, and excitation power 0.1–100 μ W. In the known ordering-induced low energy emission band we resolve narrow optical transition lines with 0.3–1.0 meV width. They show no thermal broadening, a diamagnetic shift with pronounced anisotropy, and biexcitonic states. We demonstrate that the transitions are connected with intrinsic quasi-zero-dimensional electron-hole confinement formed at the antiphase-boundaries in the crystal.

I. INTRODUCTION

Spontaneous long-range ordering has been observed in many ternary III-V alloy semiconductors, especially when grown with metalorganic vapor phase epitaxy (MOVPE) under appropriate conditions.¹ Most common is the CuPt_B-type ordering first observed in (GaIn)P by Gomyo *et al.*,² where alternating Ga-rich and In-rich planes are aligned in the $[111]_B$ directions. This system—which can be grown lattice matched on GaAs—is an excellent model system for understanding growth-induced ordering phenomena. (GaIn)P is also of particular interest for applications such as visible light emitter diodes,³ semiconductor lasers,⁴ and high performance tandem solar cells.⁵ The ordering can be characterized by two quantities: the degree of ordering within a given region, usually called domain, and the lateral extent of the domains. The former is quantified by the order parameter η which denotes the fraction of gallium and indium in the alternating $(111)_B$ order planes. The latter is well defined in the case of misoriented substrates, where one of the two variants of CuPt_B is selected. Here the separation of the domains is defined by antiphase boundaries (APB's), where the sequence of gallium-rich and indium-rich planes is flipped within one (or at most a few) monolayers.⁶

The ordering leads to a reduction of the band-gap energy and a valence-band splitting which can be observed in the emission of the excitonic band-to-band photoluminescence at low temperatures.^{2,7} Furthermore, an additional, ordering related low-energy emission (LE) is observed, which is characterized by (i) a large energy shift of up to 40 meV compared to the absorption peak; (ii) a linewidth of 10–20 meV, which is wider than that of disordered (GaIn)P (5 meV); (iii) a blueshift of the photoluminescence band with increasing excitation density (“moving emission”⁸); (iv) long and energy-dependent photoluminescence-decay times (up to 10 ms);⁹ (v) lateral variation of the spectral distribution on a submicrometer scale;^{10,11} and (vi) sharp emission lines appearing in microphotoluminescence spectra.^{12,13} Although this emission has up to now been attributed to spatially indi-

rect recombination,¹⁴ its structural origin is a matter of current debate.

In this paper we demonstrate that carrier confinement connected with the APB's in a partially ordered system leads to a *unique type of quantum dot* in purely bulk material.

II. EXPERIMENTS

We report on photoluminescence (PL) studies with high lateral resolution (μ -PL) on partially ordered (GaIn)P together with variation of lattice temperature, external magnetic field, and excitation density. The μ -PL resolution of less than 500 nm was achieved by a reflector based objective within a confocal setup.¹² The imaging as well as the focusing of the exciting laser was done by this objective in shared aperture mode. The samples were mounted directly on the surface of the objective. Therefore it works like an immersion objective with the refraction index of quartz. Investigation of different positions on the sample or mapping of areas was achieved by rotating two parallel quartz plates around the x and y axes, which scans the image over the pinhole of the confocal setup. Objective and sample were placed in a variable-temperature helium-flow cryostat equipped with a 12 T magnet. We dispersed the PL signal with a 0.75 m monochromator and detected it with either a photomultiplier tube or a liquid nitrogen cooled charge coupled device camera. The spectral resolution of the setup was 100 μ eV. Excitation was done by an Ar⁺ laser at 514.5 nm.

All measurements presented here were carried out on MOVPE-grown Ga_{0.52}In_{0.48}P samples with substrate misorientation of 6° towards a $[111]_B$ direction. Details of the growth procedure have been described in Ref. 15. Referring to the probed volume of ordered (GaIn)P the samples can be divided into two classes. Type A samples consist of a 1–2 μ m (GaIn)P bulk layer on GaAs substrate. The probed volume is then given by the optical spatial resolution. In order to further increase the resolution we artificially reduced the probed volume of detection by vertically as well as laterally structuring of ordered (GaIn)P. This sample, type B, consisted of a partially ordered (GaIn)P quantum well embedded

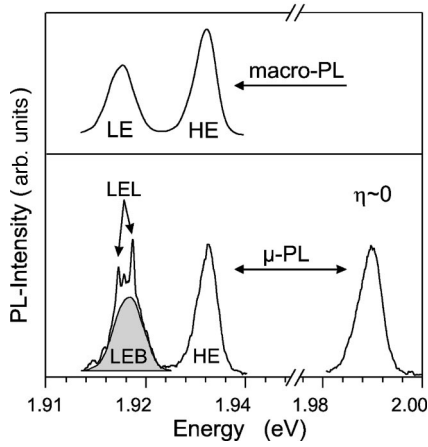


FIG. 1. Lower part: μ -PL spectra of a highly disordered ($\eta \approx 0$) and a partially ordered (GaIn)P-bulk sample. The low-energy emission splits into a broadband and superimposed narrow lines. Upper part: macro-PL spectrum of the partially ordered sample for comparison.

in (AlGa)InP barrier material, which has a band-gap difference of about 200–250 meV with respect to partially ordered (GaIn)P. The vertical structure of the type B sample consists of a 700 nm $(\text{Al}_{0.42}\text{Ga}_{0.58})\text{InP}$, a 10 nm (GaIn)P well, 10 nm $(\text{Al}_{0.42}\text{Ga}_{0.58})\text{InP}$, and a 5 nm GaAs cap layer. In addition, the 10 nm (GaIn)P layer was structured laterally via electron-beam lithography and ion implantation, which has already been described in detail elsewhere.¹⁶ This structure consists of 12 rectangular areas ($200 \times 400 \mu\text{m}$). Within each area, uniform cylinders of partially ordered (GaIn)P embedded in a disordered (GaIn)P matrix are formed. The cylinders have a periodic distance of 1 μm , a height of 10 nm, and a diameter of 55–320 nm depending on the chosen area. Within our μ -PL setup the type B sample offers the possibility to investigate *single* partially ordered (GaIn)P cylinders.

In the type A samples the degree of order ranges from $\eta \approx 0.32$ –0.5,¹⁷ and the maximum domain sizes from 50 nm up to 500 nm. The type B sample had an order parameter of $\eta \approx 0.42$ and a domain size up to 200 nm.

One important structural property of ordered (GaIn)P, especially for the unusual features we report on in this paper, are the APB's. They are aligned almost parallel to the alternating Ga-rich and In-rich order planes, which is along the $[111]_B$ -direction. Therefore, in as-grown samples, the APB's lay under an angle of about 50° with respect to the $[001]$ surface plane. In order to apply a magnetic field parallel and perpendicular to the planes of APB's two pieces of one type A sample were bevel polished. In these samples APB's are in turn aligned almost parallel or perpendicular to the sample surface, respectively, i.e., $\vec{B} \parallel \text{APB}$ and $\vec{B} \perp \text{APB}$.

III. RESULTS

A. Narrow emission lines in μ -PL

First we present the experimental results on the type A bulk samples and concentrate on the characterization of the unique feature we found in μ -PL. For comparison, Fig. 1 shows in the upper part a typical macro-PL spectrum of partially ordered (GaIn)P ($\eta \approx 0.32$). The low-energy emission

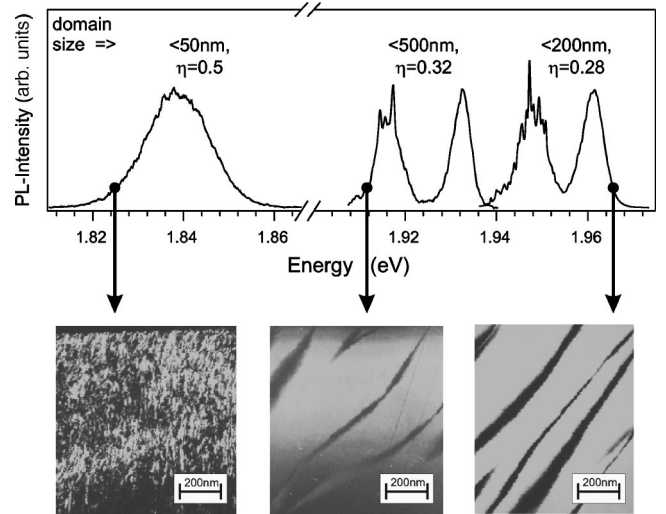


FIG. 2. μ -PL spectra of partially ordered samples with different domain sizes and degrees of order. Also shown are the related TEM's.

(LE) of this spectrum is the ordering induced PL, the high-energy emission (HE) is the excitonic band to band transition. In the lower part of Fig. 1 (left hand side) a typical μ -PL spectrum of the same sample is presented. In contrast to macro-PL, high spatially resolved spectra show that the LE consists of two parts: a broad underlying PL-band (shaded area) and superimposed *narrow emission lines*.

On the right hand side of the lower part of Fig. 1 we see a μ -PL spectrum of a disordered sample. These samples did not show any sharp features. Narrow emission lines have only been observed in partially ordered samples with μ -PL. The lines have a Lorentzian shape with full width at half maximum (FWHM) of 0.3–1.0 meV.

In order to make discussion easier we introduce the following abbreviations for the different parts of the PL spectra seen in Fig. 1: (i) HE, which is found in macro- as well as in μ -PL, (ii) LEL for the new narrow low energy emission lines, and (iii) LEB for the broad low-energy emission band.

In the following part we further concentrate on the origin and nature of LEL and LEB. At this point we want to emphasize that the broad PL band in the low-energy regime does not consist of unresolved narrow lines. Instead, there are two different kinds of transitions in the same energy range. This can be directly seen from the magnetic-field dependent measurements presented later in this paper.

B. Correlation of the number of LEL to APB density

Partially ordered (GaIn)P is mainly characterized by the order parameter η and the domain size or the density of APB's within a given probed volume. In order to search for correlation of the LEL with these parameters we investigate type A samples with different η and different APB density. The latter is taken from transmission electron micrograph (TEM) images. Fig. 2 summarizes the results.

First, the energetic position of the spectra reflects the degree of order. A high-order parameter η corresponds to a large value of band-gap reduction and for that reason shifts the spectra to lower energies. But if we concentrate on the number of LEL a dependence on the density of APB's is

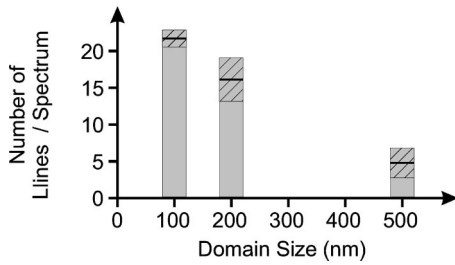


FIG. 3. Relation between the number of narrow emission lines per spectrum and the maximum domain size for different samples. The shaded area represents the variation of the values taken from 30 spectra of each sample.

found while we did not find a systematic dependence on η . For samples with a low APB density, with a domain size <500 nm (Fig. 2 in the middle) only a few LEL are observed. If the APB density increases the number of LEL increase, too, as can be seen on the right-hand side from the spectrum of a sample with a domain size <200 nm. For a sample with domains <50 nm (left-hand side) there is still a structure in the PL signal, but single narrow emission lines cannot be resolved any more. A systematic study of 30 spectra of each sample type is shown in Fig. 3. We clearly see that the number of LEL increases with increasing APB density or decreasing domain size. From these analyses we can conclude that the existence of LEL is linked to the APB's and that there is no relation to η .

C. Temperature dependence

To investigate the nature of the LEL we compared their thermal broadening with that of the LEB (determined from a Gaussian fit) via heating of the crystal from 3 K to 60 K. These measurements are shown in Fig. 4. In striking contrast to the LEB the narrow LEL do not show any broadening for lattice temperatures up to 60 K within an accuracy of ± 0.1 meV. This is an unambiguous spectroscopic evidence for a fully confined *zero-dimensional system*, having a δ -function-like electronic density of states.

This is proof that LEL and LEB belong to different types of transitions in the same energy range, as mentioned before.

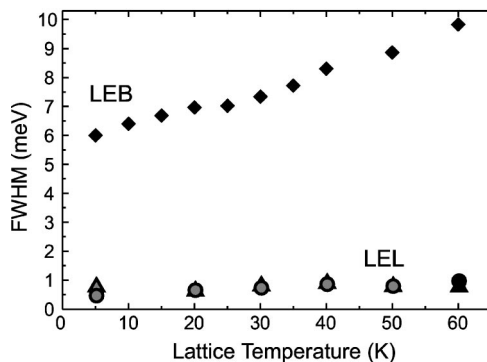


FIG. 4. Thermal broadening of the low-energy broadband emission (LEB) and the narrow low-energy lines (LEL). The latter show no thermal broadening, which is evidence for a δ -like density of states.

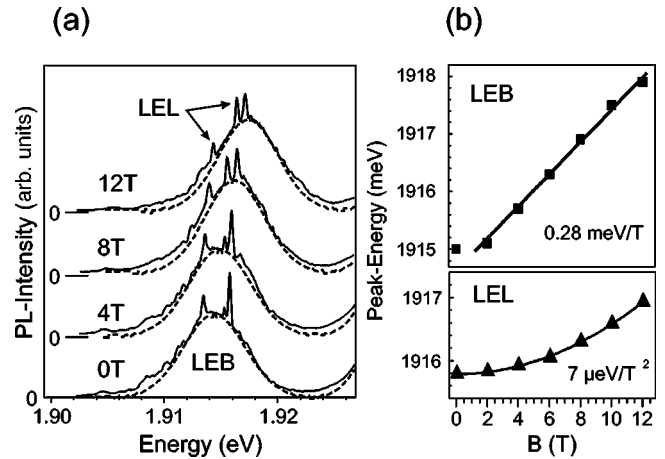


FIG. 5. (a) μ -PL spectra in the presence of an external magnetic field along the growth direction. (b) Top: peak energy of a Gaussian fit to the low-energy broadband emission [LEB, dashed lines in (a)] versus B field; bottom: energy for a narrow low-energy line (LEL), the solid line is a parabolic fit with the indicated curvature.

D. Magnetic-field dependence

To get further information about the system we performed magneto μ -PL from 0 T to 12 T at low temperatures of 3 K. The experiments for ordered bulk (GaIn)P samples with a maximum domain size >100 nm are summarized in Fig. 5. In (a) a typical spectrum for four different magnetic fields in the LE energy range is shown. The peak energy of the LEB (dashed lines) is plotted in (b), top, and for a narrow emission line of the same spectra in (b), bottom. Here we see most clearly that there are two different kinds of transitions in the same energy range: while the LEB shows a strong almost linear shift the LEL have a fully excitonic behavior that can be fitted with the quadratic function $f(x) = ax^2 + b$. The mean value of this diamagnetic shift for about 30 different narrow lines amounts to $a = 7(\pm 2) \mu\text{eV}/\text{T}^2$.

The linear B dependence of the LEB indicates the behavior of a quasifree carrier in a magnetic field and can be described by Landau's formula: $\Delta E = (\mu_B/m_r)B$ with $m_r = m^*/m_0$, the electron mass m_0 , the Bohr magneton $\mu_B = 57.88 \mu\text{eV}/\text{T}$, and the effective carrier mass m^* . If we calculate m^* from the experimental value of the slope, $0.28 \text{ meV}/\text{T}$ we get $m^* = 0.20m_0$. This is in good agreement with the calculated valence-band mass $m_v^* = 0.21m_0$ of (GaIn)P by Jones *et al.*¹⁸ It can be interpreted as only the holes are responsible for the Landau-like magnetic-field dependence. That is, the holes are quasifree carriers, whereas the electrons feel strong structural confinement like local potential minima, restricting the electron cyclotron motion.

E. Zeeman-splitting

The external B field leads for some of the narrow emission lines to a Zeeman splitting linearly with B into two lines [Fig. 6(a)]. In this case of energy splitting due to spin a circular polarization dependence of PL is expected and can be observed in our measurements in Fig. 6(a), shown at 8 T. The lower transition is σ^- and the higher transition σ^+ circular polarized in agreement with the quantum dot system of Heller and Bockelmann.¹⁹ The energy splitting versus

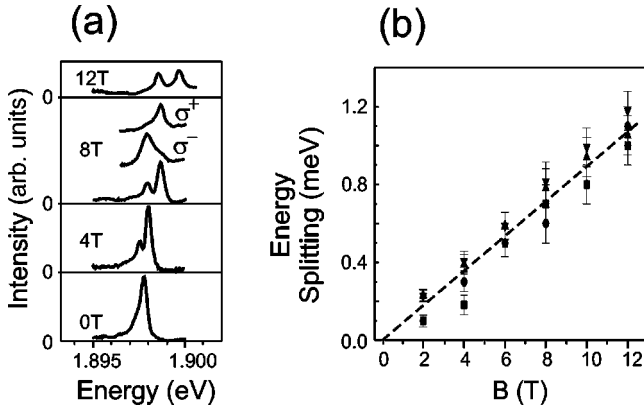


FIG. 6. Zeeman splitting of a LEL. (a) Spectra of a LEL for different magnetic fields. At the 8 T spectrum the difference of the two transitions with respect to circular polarization is shown. (b) Linear dependence of the splitting for four different LEL's with a mean value of $90 \mu\text{eV}$.

magnetic field for four different transitions is plotted in Fig. 6(b). The best linear fit to the data has a slope of $90(\pm 4) \mu\text{eV/T}$. This splitting corresponds to an effective exciton g factor of 1.5.¹⁹

From the experimental findings so far we deduce that for LEL the transitions are due to excitonic quasi-zero-dimensional states spatially connected with the APB's.

F. B-field anisotropy

We performed magneto μ -PL measurements up to 12 T at low temperatures (3 K) by applying the magnetic field in different directions with respect to the APB's. The results are summarized in Fig. 7.

In Figs. 7(a), 7(b), and 7(c) the energetic peak positions of the narrow LEL are plotted vs the magnetic field, which is directed at an angle of $\approx 50^\circ$, parallel, and perpendicular, to the APB's, respectively. The B -field orientation with respect to APB's was achieved by using bevel-polished samples and is sketched in Fig. 7 (lower right). In all three

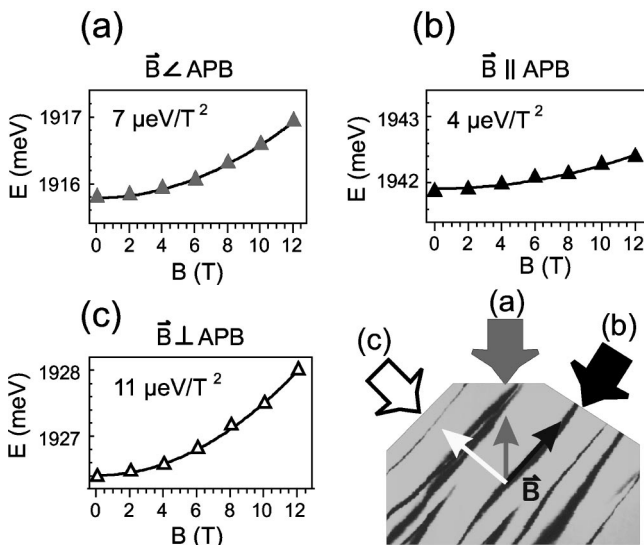


FIG. 7. Diamagnetic shift for different orientations of the applied magnetic field with respect to the APB's.

different configurations we observe a purely diamagnetic shift, but with different curvature. With increasing angle between B -field and APB orientation (0° for $\text{APB} \parallel \vec{B}$) the value of diamagnetic shift increases from $11(\pm 2) \mu\text{eV/T}^2$ to $4(\pm 1) \mu\text{eV/T}^2$ for the perpendicular [(c), $\text{APB} \perp \vec{B}$] to the parallel [(b), $\text{APB} \parallel \vec{B}$] case, respectively.

The anisotropic diamagnetic shift can be interpreted from two points of view: (i) by means of anisotropic effective masses or (ii) anisotropic geometry of the above-mentioned quantum dots. The first model assumes the optical transition to be dominantly effected by the barrier material $\text{Ga}_{1-x}\text{In}_x\text{P}$. Theoretical²⁰ and experimental²¹ investigations show that the ordering of (GaIn)P induces a strong anisotropy of the effective masses. Taking $\eta=0.5$ into account the ratio of the effective masses parallel and perpendicular to the APB's is ≈ 1.3 . This in turn could explain the ratio of the diamagnetic shift of ≈ 2.7 .

Besides anisotropic effective masses an anisotropy of the geometry of quantum dots (QD's) could explain the observed diamagnetic shifts. Calculations on diamagnetic shift of quantum dot systems by Halonen *et al.*²² show that a confinement potential leads to a weakening of the influence of magnetic field on line shifts. Experimentally this has been observed by Zrenner *et al.* in quantum-well geometries²³ and by Wang *et al.* in self-assembled quantum dots.²⁴

The intrinsic QD investigated here were shown to be connected to APB's, i.e., to Ga- or In-rich regions. Based on this fact the second model assumes that the optical transition is dominated by the dot material, leading to zinc-blende-like effective masses for the carriers.

In this framework the anisotropic diamagnetic shift can be interpreted consistently by a QD with weaker confinement within the APB plane than perpendicular to it. This picture of a disk-shaped QD is supported by TEM studies²⁵ which have shown that the APB's are mostly two-dimensional structures aligned along $[\bar{1}12]$ and curved irregularly with a preference along (110).

G. Excitation density dependence: Biexcitonic transitions

The type A samples studied so far are bulk material. For this reason the probed volume is determined by the spatial resolution of the setup. In our experiments this resolution is diffraction limited and the minimal probed volume is restricted to $\approx (500 \text{ nm})^3$.

For the investigation of the dependence of the LEL on excitation density we have to address the problem that the underlying LEB dominates the spectra for stronger excitation densities, whereas the LEL saturates and cannot be resolved above the LEB PL signal. To minimize the LEB PL signal we artificially reduced the probed volume of partially ordered material to cylindrically structured areas of 10 nm height and a diameter of 55–320 nm. These are the type B samples described above. The influence of structuring on the qualitative appearance of the spectra can be neglected.²⁶ With our high lateral resolution of 500 nm we are able to address single structured cylinders.

A typical spectrum of such a single cylinder and its dependence on excitation density is shown in Fig. 8(a). At very weak excitation only one transition line is observed (circles). With increasing excitation density new lines develop on the

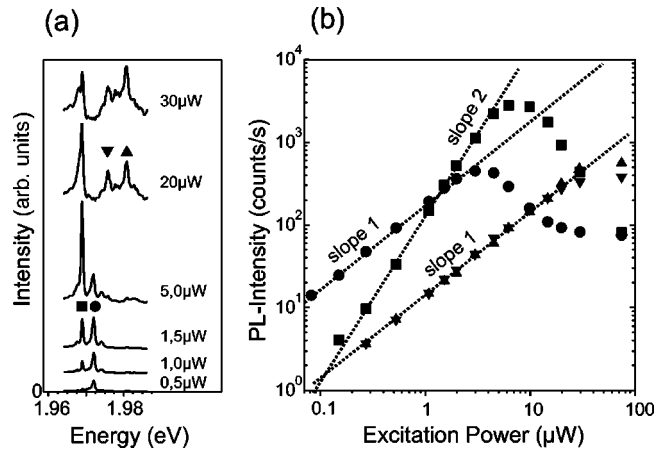


FIG. 8. Dependence on excitation density: (a) full spectra and (b) peak intensities in a double logarithmic plot. Slope 2 for the low-energy transition (squares) indicates a biexcitonic state.

high-energy side (triangles). They are spaced equidistantly to each other within an accuracy of $200 \mu\text{eV}$. However, for various positions on the sample the value of this spacing varies in the range of $2\text{--}4 \text{ meV}$. A series of spectra of single cylinders from different patches is plotted in Fig. 9. The PL line which is marked by a black arrow is the line that develops first with increasing excitation density.

The observed, clearly nonstatistic energetic distribution of the lines which are almost equidistant and the way the spectrum develops with increasing excitation density starting with a single transition line leads to the assumption that we observe spectra of individual, *single quantum disks*. We then attribute the first line to the transition from the lowest lying electron-hole excited state to the crystal ground state and the higher-energy lines to transitions from higher excited states of the same confinement region. This behavior is comparable with recently reported results on the excitation density dependence of single $\text{GaAs}/\text{Al}_x\text{Ga}_{1-x}\text{As}$ and $\text{InAs}/\text{Al}_x\text{Ga}_{1-x}\text{As}$ quantum dot spectra of Bockelmann *et al.* and Dekel *et al.*, respectively.^{27,28}

In Fig. 8(a), also on the low-energy side of the first line, another line develops (squares) and exceeds the former in intensity. Its peak intensity versus excitation density increases with slope 2 in the double logarithmic plot [Fig. 8(b)], whereas all other lines show slope 1 behavior. This

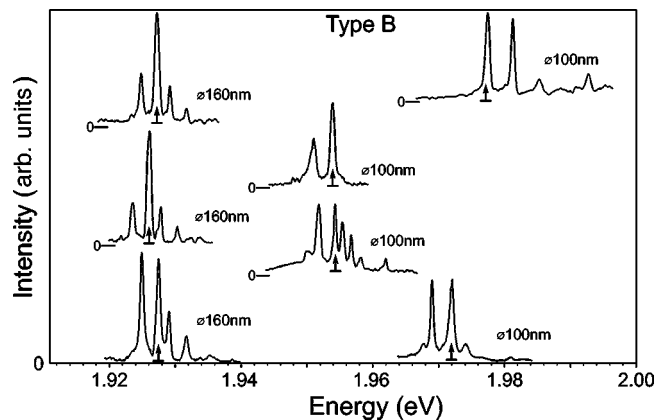


FIG. 9. μ -PL spectra of different single cylinder structures of partially ordered $(\text{GaIn})\text{P}$ in sample type B.

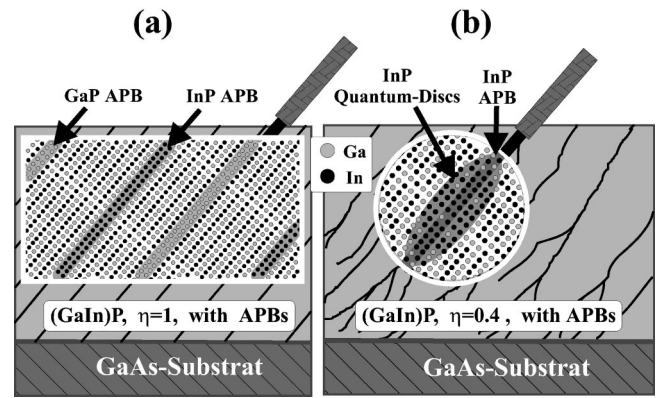


FIG. 10. Model for the occurrence of quantum disks at InP APB. (a) Ideally ordered crystal with double layers of InP and GaP. (b) Development of an InP disklike structure due to disorder.

quadratic dependence of emission intensity on excitation density is the typical characteristic of a biexcitonic transition observed in many confined systems,^{29,30} and the difference in transition energy of typically 3 meV with respect to the electron-hole excited state is a plausible value for the biexciton binding energy. From measurements on GaAs -bulk, -quantum wells, and -quantum dots we know that the confinement of excitons leads to a significant increase of biexciton binding energy.³⁰ Therefore, biexcitonic states become an important elementary excitation of a zero-dimensional system.^{28,30,31} As can be seen from Fig. 9, almost every single cylinder spectrum shows such a biexcitonic transition line lying on the low-energy side of the first transition (marked by black arrow).

Due to the connection of LEL to the APB's we conclude that every single structured cylinder which shows a spectrum like those of Fig. 9 is crossed by an APB, and the PL lines are the transitions of a single quantum disk located at this APB. Indeed TEM images presented elsewhere¹⁶ of a comparable structured sample, grown with the same parameters, show that almost every ordered area is crossed by an APB. But also a few cylinders with no APB are existent. These remain dark in a PL map.¹²

IV. DISCUSSION

The magneto μ -PL experiments clearly show the existence of confinement potentials located at the APB's in a partially ordered alloy semiconductor. This is consistent with the following model of the microstructure of this material (Fig. 10): In an ordered $(\text{GaIn})\text{P}$ crystal an APB is a double layer of one of both cations. Therefore two types of APB's can exist, Ga and In APB's [Fig. 10(a)]. An In-APB in an ideally ordered crystal can be seen as a two monolayer InP quantum well in $(\text{GaIn})\text{P}$ barrier material aligned in $[111]_B$ direction. In partially ordered crystals the given quantum well would show thickness fluctuations due to the finite degree of ordering which introduces Ga in the In-rich planes, generating disklike islands of InP [Fig. 10(b)]. This geometry is comparable to thin $\text{GaAs}/\text{Al}_x\text{Ga}_{1-x}\text{As}$ quantum wells, where several authors have shown the existence of naturally formed quantum disks due to thickness fluctuation of the $1\text{--}3$ monolayer thick GaAs layer.^{23,32,33}

Even more closely related to our model of InP-quantum

wells represented by APB's in (GaIn)P is the system of InP–Stranski-Krastanow dots grown on (GaIn)P. In the regions between the fully developed pyramidal dots a remaining InP wetting layer with a mean thickness of a few monolayers exists. Its thickness fluctuations also lead to naturally formed quantum dots and to sharp emission lines in the PL spectra which have been observed in optical experiments³⁴. The above-mentioned model is based only on general structural properties of partially ordered ternary semiconductors. Therefore we expect the described optical features to occur in other III-V compounds as well.

V. SUMMARY

To summarize, we have performed μ -PL experiments on partially ordered (GaIn)P-bulk samples. We found that for

high spatial resolution the known LE luminescence splits into a broad emission band, LEB, and superimposed narrow emission lines, LEL. The latter can be characterized by (i) a FWHM of 0.3 to 1.0 meV, (ii) no thermal broadening up to 60 K, (iii) an anisotropic diamagnetic shift, (iv) the existence of biexcitonic states with a typical binding energy of 3 meV, and (v) Zeeman splitting of $+90 (\pm 4) \mu\text{eV/T}$. We attribute these narrow emission lines to zero-dimensional InP quantum discs naturally formed at In-In antiphase boundaries embedded in (GaIn)P.

ACKNOWLEDGMENT

We thank E. Spiecker for valuable discussions and his sample surface preparation for the magnetic-field orientation experiments.

-
- ¹A. Zunger and S. Mahajan, in *Handbook on Semiconductors*, edited by T.S. Moss (Elsevier, Amsterdam, 1994), p. 1399.
- ²A. Gomyo, K. Kobayashi, S. Kawata, I. Hino, and T. Suzuki, *J. Cryst. Growth* **77**, 367 (1986).
- ³E. Greger, K. H. Gulden, P. Riel, H. P. Schweizer, M. Moser, G. Schmiedel, P. Kiesel, and G. H. Döhler, *Appl. Phys. Lett.* **68**, 2383 (1996).
- ⁴D. P. Bour, in *Quantum Well Lasers*, edited by P. S. Zory (Academic Press, Boston, 1993), p. 415.
- ⁵K. A. Bertness, S. R. Kurtz, D. J. Friedman, A. E. Kibbler, C. Kramer, and J. M. Olson, *Appl. Phys. Lett.* **65**, 989 (1994).
- ⁶L. C. Su, I. H. Ho, and G. B. Stringfellow, *J. Appl. Phys.* **75**, 5135 (1994).
- ⁷A. Mascarenhas, S. Kurtz, A. Kibbler, and J. M. Olson, *Phys. Rev. Lett.* **63**, 2108 (1989).
- ⁸M. C. DeLong, P. C. Taylor, and J. M. Olson, *Appl. Phys. Lett.* **57**, 620 (1990).
- ⁹P. Ernst, C. Geng, F. Scholz, and H. Schweizer, *Phys. Status Solidi B* **193**, 213 (1996).
- ¹⁰M. J. Gregor, P. G. Blome, R. G. Ulbrich, P. Grossmann, S. Grosse, J. Feldmann, W. Stolz, E. O. Göbel, D. J. Arent, M. Bode, K. A. Bertness, and J. M. Olson, *Appl. Phys. Lett.* **67**, 3572 (1995).
- ¹¹S. Smith, H. M. Cheong, B. D. Fluegel, J. F. Geisz, J. M. Olson, L. L. Kazmerski, and A. Mascarenhas, *Appl. Phys. Lett.* **74**, 706 (1999).
- ¹²U. Kops, R. G. Ulbrich, M. Burkhard, C. Geng, F. Scholz, and H. Schweizer, *Phys. Status Solidi A* **164**, 459 (1997).
- ¹³H. M. Cheong, A. Mascarenhas, J. F. Geisz, J. M. Olson, M. W. Keller, and J. R. Wendt, *Phys. Rev. B* **57**, R9400 (1998).
- ¹⁴M. C. DeLong, W. D. Ohlsen, I. Viohl, P. C. Taylor, and J. M. Olson, *J. Appl. Phys.* **70**, 2780 (1991).
- ¹⁵C. Geng, A. Moritz, S. Heppel, A. Mühe, J. Kuhn, P. Ernst, H. Schweizer, F. Phillipp, A. Hangleiter, and F. Scholz, *J. Cryst. Growth* **170**, 418 (1997).
- ¹⁶M. Burkhard, C. Geng, A. Mühe, F. Scholz, and H. Schweizer, *Appl. Phys. Lett.* **70**, 1290 (1997).
- ¹⁷These values were extracted from the valence-band splitting measured by photoluminescence excitation spectroscopy and the calculations in S.-H. Wei, D. B. Laks, and A. Zunger, *Appl. Phys. Lett.* **62**, 1937 (1993).
- ¹⁸E. D. Jones, D. M. Follstaedt, H. Lee, J. S. Nelson, R. P. Schneider, R. G. Alonso, G. S. Horner, J. Machol, and A. Mascarenhas, in *Proceedings of the 22nd International Conference on the Physics of Semiconductors*, edited by D. J. Lockwood (World Scientific, Singapore, 1995), p. 293.
- ¹⁹W. Heller and U. Bockelmann, *Phys. Rev. B* **55**, R4871 (1997).
- ²⁰A. Franceschetti, S.-H. Wei, and A. Zunger, *Phys. Rev. B* **52**, 13992 (1995).
- ²¹P. Ernst, Y. Zhang, F. A. J. M. Driessen, A. Mascarenhas, E. D. Jones, C. Geng, F. Scholz, and H. Schweizer, *J. Appl. Phys.* **81**, 2814 (1997).
- ²²V. Halonen, T. Chakraborty, and P. Pietiläinen, *Phys. Rev. B* **45**, 5980 (1992).
- ²³A. Zrenner, L. V. Butov, M. Hagn, G. Abstreiter, G. Böhm, and G. Weimann, *Phys. Rev. Lett.* **72**, 3382 (1994).
- ²⁴P. D. Wang, J. L. Merz, S. Farad, R. Leon, D. Leonard, G. Medeiros-Ribeiro, M. Oestreich, P. M. Petroff, K. Uchida, N. Miura, H. Akiyama, and H. Sakaki, *Phys. Rev. B* **53**, 16458 (1996).
- ²⁵E. Spiecker, M. Seibt, W. Schröter, M. Wenderoth, R. Winterhoff, C. Geng, and F. Scholz, in *Microscopy of Semiconducting Materials 1999*, edited by A. G. Cullis and R. Beau (Institute of Physics and Physical Society, London, in press).
- ²⁶The lateral confinement of a 100–320 nm square potential well with disordered (GaIn)P as barrier material is less than 1 meV and can be neglected. The quantization energy in growth direction coming from the 10 nm quantum well only leads to a slight shift of the energetic position of 6 meV. M. Burkhard, A. Engler, C. Geng, F. Scholz, and H. Schweizer, in *Optoelectronic Materials: Ordering, Composition Modulation, and Self-Assembled Structures*, edited by E. D. Jones, A. Mascarenhas, and P. Petroff, MRS Symposia Proceedings No. 417 (Materials Research Society, Pittsburgh, 1995), p. 67.
- ²⁷U. Bockelmann, Ph. Roussignol, A. Filoramo, W. Heller, G. Abstreiter, K. Brunner, G. Böhm, and G. Weimann, *Phys. Rev. Lett.* **76**, 3622 (1996).
- ²⁸E. Dekel, D. Gershoni, E. Ehrenfreund, D. Spektor, J. M. Garcia, and P. M. Petroff, *Phys. Rev. Lett.* **80**, 4991 (1998).
- ²⁹J. C. Kim, D. R. Wake, and J. P. Wolfe, *Phys. Rev. B* **50**, 15099 (1994).
- ³⁰K. Brunner, G. Abstreiter, G. Böhm, G. Tränkle, and G.

- Weimann, Phys. Rev. Lett. **73**, 1138 (1994).
- ³¹U. Woggon, *Optical Properties of Semiconductor Quantum Dots* (Springer, Berlin, 1997).
- ³²H. F. Hess, E. Betzig, T. D. Harris, L. N. Pfeiffer, and K. W. West, Science **264**, 1740 (1994).
- ³³D. Gammon, E. S. Snow, B. V. Shanabrook, D. S. Katzer, and D. Park, Phys. Rev. Lett. **76**, 3005 (1996).
- ³⁴L. Samuelson, N. Carlsson, P. Castrillo, A. Gustavsson, D. Hessmann, J. Lindahl, L. Montelius, A. Peterson, M.-E. Pistol, and W. Seifert, Jpn. J. Appl. Phys., Part 1 **34**, 4392 (1995).